Electronic Supplementary Material (ESI) for Dalton Transactions.

Free-standing manganese cobalt sulfide@cobalt nickel layered double hydroxide core-shell heterostructure for asymmetric supercapacitor

Haoyan Liang, Tiesong Lin, Shengyao Wang, Henan Jia, Chun Li, Jian Cao, Jicai Feng, Weidong Fei and Junlei Qi*

State Key Laboratory of Advanced Welding and Joining, Harbin Institute of Technology, Harbin 150001, China

*Corresponding authors: Tel. /fax: 86-451-86418146;

E-mail: jlqi@hit.edu.cn (J. Qi)

Experimental

Growth of $MnCo_2S_4$ nanotube arrays

All the reagents were purchased in analytical grade without further purification. The Ni foam (2 cm × 5 cm) was cleaned in 10% HCl solution to remove the oxide layer. Then, it was rinsed with ethanol and deionized water under the ultrasonic treatment. The $MnCo_2S_4$ nanotube arrays were synthesized by a two-step hydrothermal reaction. Typically, 0.3958 g $MnCl_2 \cdot 4H_2O$, 1.1641 g $Co(NO_3)_2 \cdot 6H_2O$, 0.7207 g urea and 0.3704 g NH_4F were dissolved in 80 mL deionized water to form a homogeneous solution under the magnetic stirring for 20 min. Then, the cleaned Ni foam was immersed into the solution and transferred to a 100 mL Teflon-lined stainless-steel autoclave. The hydrothermal reaction was conducted under 120 °C and kept for 12 h. The MnCo-precursors were rinsed with deionized water and ethanol for several times and dried at 60 °C for 8 h under the vacuum condition.

The MnCo-precursors were transferred to the 100 mL Teflon-lined stainless steel autoclave with 0.01M Na_2S solution and maintained at 160 °C for 6 h. After cooled to the room temperature, the $MnCo_2S_4$ nanotube arrays were washed with deionized water and ethanol, and dried under vacuum at 60 °C for further use. The mass loading was determined to be ~2 mg cm^{-2}.

Synthesis of $MnCo_2S_4$@CoNi LDH (MCS@CN LDH) core-shell nanostructure

The synthesis of $MnCo_2S_4$@CoNi LDH core-shell nanostructure was conducted through a potentiostaic electrodeposition as previous reported. In a typical procedure, the electrodeposition are used in a three-electrode system, by using $MnCo_2S_4$

nanotube arrays substrate as the working electrode, the Pt as the counter electrode and Ag/AgCl as the reference electrode. The electrolyte are containing 0.15 M $CoCl_2 \cdot 6H_2O$ and 0.15 M $Ni(NO_3)_2 \cdot 6H_2O$. The electrodeposition was carried out at a constant potential of -1.0 V *vs.* Ag/AgCl. The electrode was rinsed with deionized water and ethanol, and dried at 60 °C overnight. The mass loading of the electrode after the electrodeposition was ~4 mg cm^{-2}.

Synthesis of N-doped rGO (N-rGO)

Typically, 90 mg GO was dispersed in 48 mL deionized water with ultrasonicating for 2 h to form a homogeneous solution. 32 mL N,N-Dimethylformamide (DMF) was poured into the solution under continuous stirring for another 1 h. Then, the solution was transferred into a 100 mL Teflon-lined stainless autoclave and maintained at 180 ^{o}C for 12 h. Finally, the sample was rinsed with deionized water and dried by freeze-drying.

Materials Characterization

The morphology and nanostructure of the samples were characterized by SEM (Helios Nanolab 600i and Merlin Compact) and TEM (Tecnai G2 F30), respectively. XRD was performed using X'PERT and D/max 2550. Surface chemical properties were investigated by XPS (ESCLAB 250Xi)

Electrochemical measurements

The electrochemical measurements were conducted using a three-electrode cell, where Pt was used as the counter and Hg/HgO as reference electrodes in 6.0 M KOH electrolyte. Cyclic voltammetry (CV), galvanostatic charge/discharge (GCD) curves and electrochemical impedance spectroscopy (EIS) were carried out on an electrochemical workstation (CHI760E). The EIS analysis is conducted over a frequency ranging from 100 kHz to 0.01 Hz with amplitude of 5 mV. The negative electrode was composed of N-rGO, carbon black and PVDF with a mass ratio of 8:1:1. The mixture was coated on the Ni foam uniformly and dried at 120 ^{o}C for 3 h. The asymmetric supercapacitor (MCS@CN LDH//N-rGO) were tested in a two-electrode system. The mass ratio of the positive and the negative were calculated by the following equation:

$$m+/m- = (C- \times \Delta E-)/(C+ \times \Delta E+)$$

Where m is the mass, C is the specific capacitance and ΔE is the potential of the electrode materials.

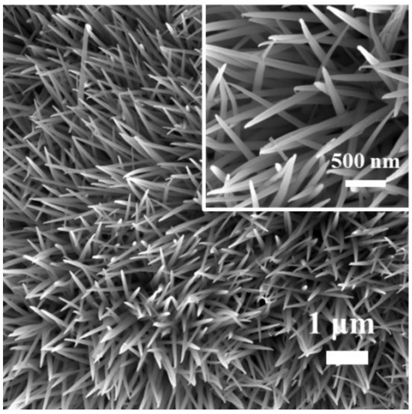

Fig. S1 The SEM image of MnCo precursor on Ni Foam.

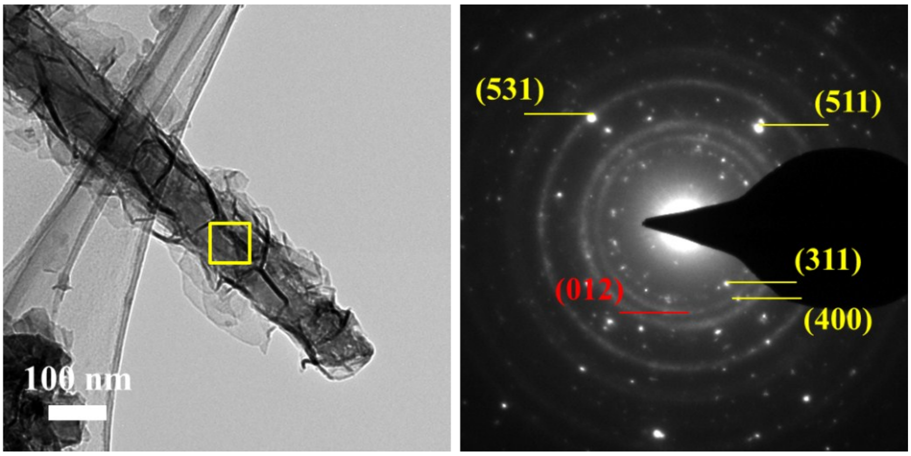

Fig. S2 The SAED image of MCS@CN LDH.

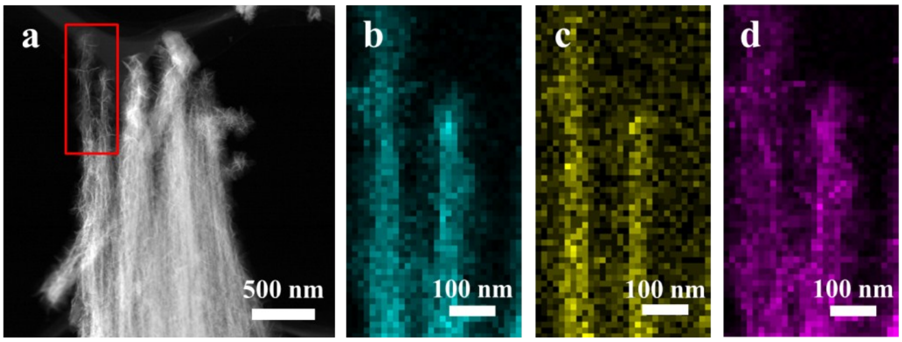

Fig. S3 (a) The HAADF image of MCS@CN LDH and EDS mapping of (b) Co, (c) Mn and (d) Ni.

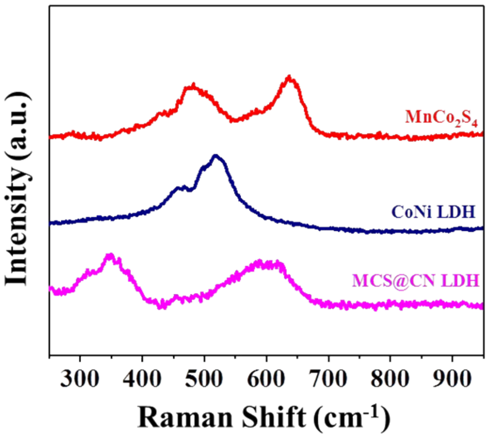

Fig. S4 Raman spectroscopy of $MnCo_2S_4$, CoNi LDH and MCS@CN LDH.

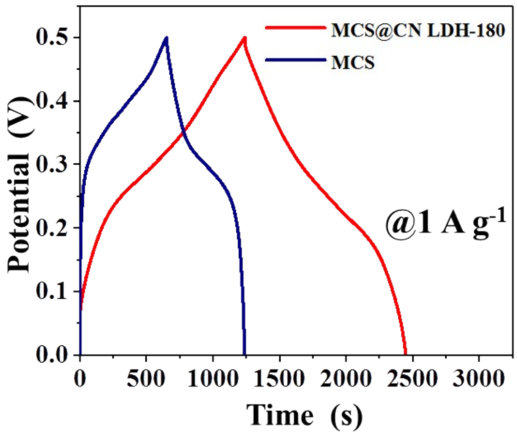

Fig. S5 The comparison of GCD curve between two electrodes at 1 A g^{-1}.

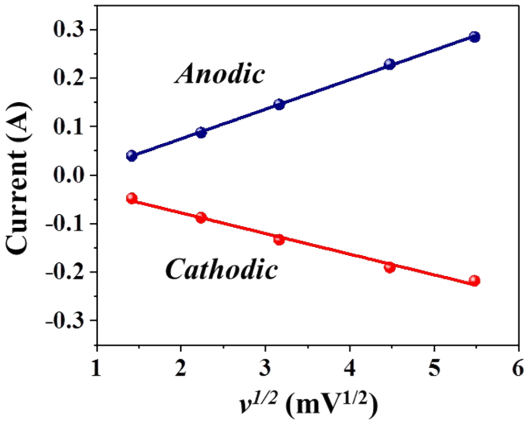

Fig. S6 The i_p-v plot of MCS@CN LDH nanostructure.

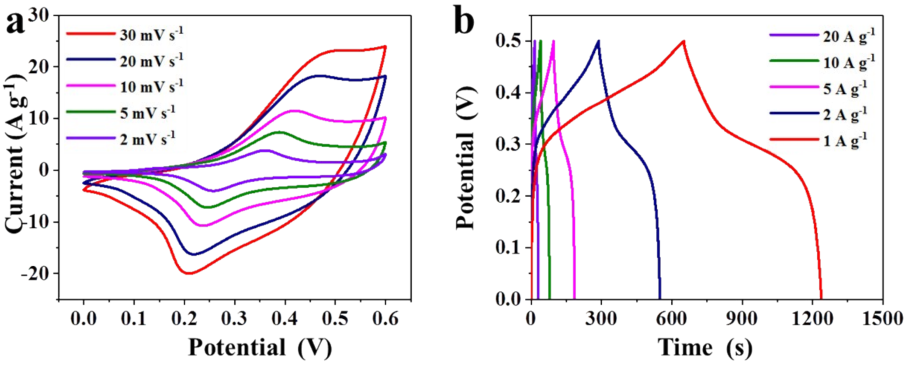

Fig. S7 Electrochemical performance of $MnCo_2S_4$ nanotubes (a) CV curves at different scan rates and (b) GCD curves at different current densities.

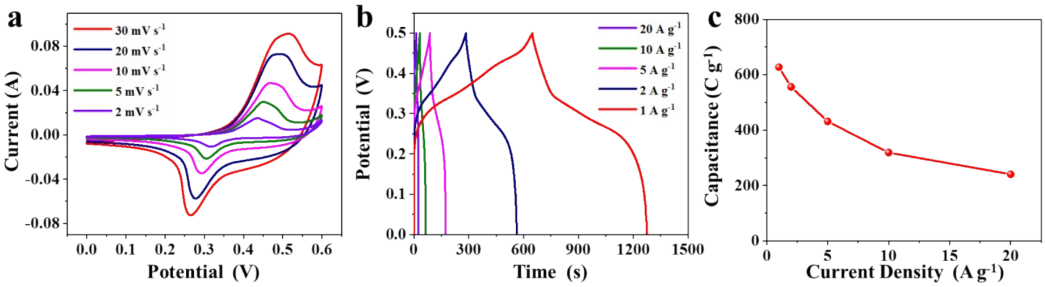

Fig. S8 Electrochemical performance of NiCo LDH nanosheets (a) CV curves at different scan rates, (b) GCD curves at different current densities and (c) specific capacitance.

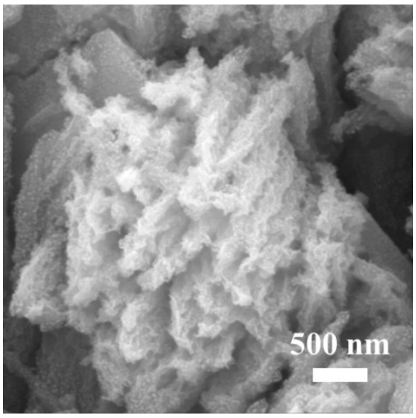

Fig. S9 SEM image of MCS@CN LDH after 10000 cycles.

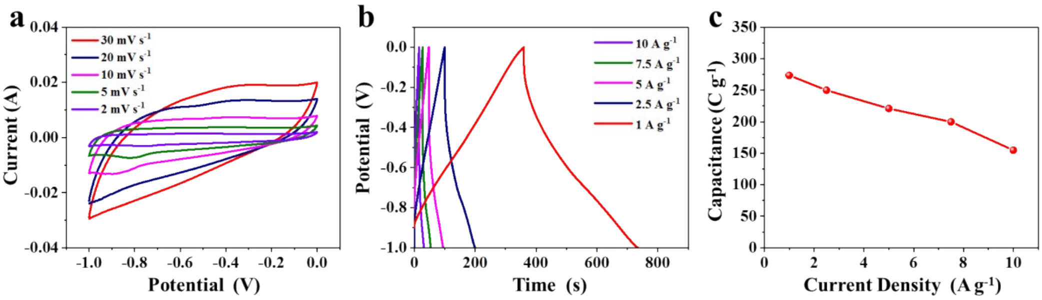

Fig. S10 Electrochemical performance of N-rGO electrode. (a) CV curves at different scan rates, (b) GCD curves at different current densities and (c) Specific capacitance.

Table S1 Comparison of specific capacitance with similar reports

Electrode materials	Specific capacitance	Ref.
KCu_7S_4@NiMn LDHs	733.8 F g^{-1} at 1 A g^{-1}	1
$NiCo_2S_4$@NiMn LDH	1740 mF cm^{-2} at 1 mA cm^{-2}	2
$MnCo_2S_4$/NSG	1324.3 F g^{-1} at 1 A g^{-1}	3
$MnCo_2S_4$ core-shell	2067 F g^{-1} at 1 A g^{-1}	4
Co_9S_8@Ni-Co LDH	1020 C g^{-1} at 1.25 A g^{-1}	5
$NiCo_2S_4$/Ni-Co LDH	1765 F g^{-1} at 1 A g^{-1}	6
CoS_x/Ni-Co LDH	1562 F g^{-1} at 1 A g^{-1}	7
CoAl-LDH/$NiCo_2S_4$	760 C g^{-1} at 1 A g^{-1}	8
$MnCo_2S_4$@CoNi LDH	1206 C g^{-1} (2412 F g^{-1}, 9.8 F cm^{-2}) at 1 A g^{-1} (4 mA cm^{-2})	This work

References

1. X. L. Guo, J. M. Zhang, W. N. Xu, C. G. Hu, L. Sun and Y. X. Zhang, *J. Mater. Chem. A*, 2017, **5**, 20579-20587.

2. H. Wan, J. Liu, Y. Ruan, L. Lv, L. Peng, X. Ji, L. Miao and J. Jiang, *ACS Appl. Mater. Interfaces*, 2015, **7**, 15840-15847.

3. H. Wang, K. Zhang, Y. Song, J. Qiu, J. Wu and L. Yan, *Carbon*, 2019, **146,** 420-429.

4. S. Liu and S. C. Jun, *J. Power Sources*, 2017, **342**, 629-637.

5. H. Jia, Z. Wang, X. Zheng, J. Lin, H. Liang, Y. Cai, J. Qi, J. Cao, J. Feng and W. Fei, *Chem. Eng. J.*, 2018, **351**, 348-355.

6. L. Luo, B. He, W. Kong and Z. Wang, *J. Alloy Compd.*, 2017, **705**, 349-355.

7. X. Guan, M. Huang, L. Yang, G. Wang and X. Guan, *Chem. Eng. J.*, 2019, **372**, 151-162.

8. X. Zhang, S. Wang, L. Xu, T. He, F. Lu, H. Li and J. Ye, *Ceram. Inter.*, 2017, **43**, 14168-14175.